CARBON 47 (2009) 3113–3121

available at www.sciencedirect.com

ScienceDirect

journal homepage: www.elsevier.com/locate/carbon

Synthesis, characterization and optical limiting property of covalently oligothiophene-functionalized graphene material

Yongsheng Liu[a], *Jiaoyan Zhou*[a], *Xiaoliang Zhang*[b], *Zhibo Liu*[b], *Xiangjian Wan*[a], *Jianguo Tian*[b], *Tuo Wang*[a], *Yongsheng Chen*[a,*]

[a]*Key Laboratory for Functional Polymer Materials and Centre for Nanoscale Science and Technology, Institute of Polymer Chemistry, College of Chemistry, Nankai University, Tianjin 300071, China*

[b]*Key Laboratory of Weak Light Nonlinear Photonics, Ministry of Education, Teda Applied Physics School, Nankai University, Tianjin 300457, China*

ARTICLE INFO

Article history:
Received 11 June 2009
Accepted 8 July 2009
Available online 14 July 2009

ABSTRACT

An organic solution-processable functionalized graphene hybrid material with oligothiophene (6THIOP-NH-SPFGraphene) has been synthesized. The thermogravimetry analysis data shows that the hybrid is more stable than its parent graphene oxide as observed with an increased onset temperature. Ultraviolet–visible absorption and fluorescence emission data show that the attachment of the electron-acceptor group (graphene oxide sheet) onto the oligothiophene molecules results in an improved absorption than its parent compound in the whole spectral region and an efficient quenching of photoluminescence. The optical limiting properties were studied by using the open-aperture Z-scan measures at 532 nm, and the results show that 6THIOP-NH-SPFGraphene demonstrated a superior optical limiting effect, better than that of the benchmark optical limiting material C_{60}.

1. Introduction

Graphene—one-atom-thick two-dimensional (2D) layers of sp^2-hybridized carbon—exhibits remarkable electronic [1–3], optical [4,5], magnetic [6,7] and mechanical [8,9] properties that could make them useful in a variety of applications. This 2D carbon network is the fundamental building block of other carbon-based materials, such as 0D fullerenes, 1D carbon nanotubes and 3D graphite. With intensive studies for many exceptional properties and applications of several other forms of sp^2-hybridized carbon including carbon nanotube [10] and fullerene [11], it is naturally expected that graphene is prompting studies for many nanoelectronic and optoelectronic devices and as nanoscale building blocks for new nanomaterials. So far, various microelectrical devices, such as field-effect transistors [12], ultracapacitors [13], ultrasensitive sensors [14] and organic photovoltaic device [15] have been reported. But perfect graphene itself does not exist and its solubility and/or processability come as the first issue for many perspective applications of graphene-based materials. One of the most important means to further expand their potential is to functionalize their surfaces. Up to now, chemical functionalization of graphene has been focusing on improving its solubility/processability in both water and organic solvents using different soluble groups [16–19]. But solution-processable multifunctional graphene hybrid materials to take advantages of both the superior properties of graphene and the functionalizing material have been largely unexplored.

Polythiophenes and oligothiophenes possess extensive π-electron delocalization along the molecular backbone and are well known as high hole mobility materials, which makes them interesting for various optoelectronic applications [20–24]. Owing to the low resonance energy of the thiophene het-

* *Corresponding author:* Fax: +86 22 23499992.
E-mail address: yschen99@nankai.edu.cn (Y. Chen).
0008-6223/$ - see front matter
doi:10.1016/j.carbon.2009.07.027

erocycle [25–27], oligothiophenes have found utility in a wide range of nonlinear optical (NLO) materials [28–30]. Dipolar push–pull chromophores, which involve a donor and acceptor group, have been widely investigated for their NLO [31–35] and other optoelectronic properties [21,36,37]. On the other side, the presence of oxygen-containing groups in graphene oxide makes it strongly hydrophilic. But these groups can be readily used to functionalize graphene sheets. Thus, it would be expected that combining electron-donor molecules such as polythiophenes or oligothiophenes with the electron-acceptor molecule graphene would generate an interesting push–pull hybrid, potentially with good optoelectronic properties. As excellent acceptor materials like carbon nanotube and fullerene, many donor–acceptor systems based on them with excellent optoelectronic properties have been reported [38–40], but there has no report of such thiophene-based functionalized graphene material up to now. In this paper, we report the synthesis, characterization and photophysical properties of an organic solution-processable functionalized graphene (SPFGraphene) hybrid material with oligothiophene, and furthermore, a superior optical limiting property has been observed for this graphene–thiophene hybrid.

2. Experimental

2.1. Materials and reagents

All reactions and manipulations were carried out under argon (Ar) atmosphere with the use of standard Schlenk techniques. Tetrahydrofuran (THF) and diethyl ether were distilled from Na/benzophenone under Ar atmosphere. N,N,N′,N′-tetramethylethylenediamine (TMEDA) was dried over CaH and distilled. All starting materials were purchased from commercial suppliers (Alfa Aesar and Aldrich) and used without further purification. Graphene oxide was prepared using our modified Hummers method [15,44,45].

2.2. Instruments and measurements

The solution ^{1}H and ^{13}C Nuclear Magnetic Resonance (NMR) spectra were recorded on a Bruker AV400 Spectrometer. ^{13}C cross-polarisation/magic angle spinning (CP/MAS) NMR spectra were recorded on a Varian Infinity plus-400 spectrometer operating at 100.52 MHz using a 4 mm rotor spinning at 12 kHz with ^{1}H decoupling. High resolution matrix-assisted laser desorption/ionization (MALDI) spectra were collected with a Fourier transform-ion cyclotron resonance mass spectrometer instrument (Varian 7.0T FTICR-MS). Elemental analyses were performed on a Thermo Electron Flash EA 1112 elemental analyzer. Fourier transform infrared (FTIR) spectra were obtained with a Bruker TENSOR 27 instrument. All infrared (IR) samples were prepared as thin films using spectroscopic grade KBr. Raman spectra were measured by a Renishaw inVia Raman microscope at room temperature with the 514 nm line of an Ar ion laser as an excitation source. Thermogravimetry analysis (TGA) curves were recorded on a NETZSCH STA 409PC instrument under purified nitrogen gas flow with a 5 °C/min heating rate. Ultraviolet–Visible (UV–Vis) spectra were obtained with a JASCO V-570 spectrophotometer. Fluorescence spectra were obtained with a Fluoro-Max-P instrument.

The open-aperture Z-scan experiments were preformed with linearly polarized 5 ns pulses at 532 nm generated from a frequency doubled Q-switched Nd:YAG laser. The spatial profiles of the pulses are of nearly Gaussian form after the spatial filter. The pulses were split into two parts: the reflected pulse was used as reference, and we focused the transmitted pulse onto the sample by using a 25-cm focal length lens. The input pulse energy was 23 μJ. The sample was placed at the focus where the spot radius of the pulses was about 30 μm. The reflected and transmitted pulse energies were measured simultaneously with two energy detectors (Molectron J3S-10). C_{60} was employed as a standard. To compare optical limiting effect, all of the sample concentrations were adjusted to have the same linear transmittance of 65% at 532 nm in 1-mm-thick cells. For the controlled blend sample, both the solutions of 6THIOP in *o*-dichlorobenzene (ODCB) and graphene oxide in *N*,*N*-dimethylformamide (DMF) were adjusted to have the same linear transmittance of 65% at 532 nm before mixed together.

2.3. Synthesis of 2-bromo-3-octyl-5-nitrothiophene

2-Bromo-3-octylthiophene (1.0 g, 3.63 mmol) was dissolved in THF (2 ml) and acetic anhydride (4 ml) under Ar. The solution was cooled to −10 °C and a mixture of HNO_3 (65% solution, 1.66 g, 18.15 mmol) and acetic anhydride (3 ml) was added over 15 min. After stirring for 2 h, the mixture was kept in refrigerator for 12 h. An aqueous solution of NaOH (2 M, 50 ml) was added to the reaction mixture at 0 °C, and then after 30 min stirring the mixture was extracted with CH_2Cl_2 three times. The combined organic layer was washed with H_2O and brine, dried over Na_2SO_4, and evaporated under reduced pressure. The crude was purified by column chromatography (silica, petroleum ether) to obtain 2-bromo-3-octyl-5-nitrothiophene (680 mg, 2.12 mmol, 58%) as a yellow oil. ^{1}H NMR (400 MHz, $CHCl_3$): 7.64 (s, 1H), 2.57 (t, J = 7.6 Hz, 2H), 1.58 (m, 2H), 1.30 (m, 10H), 0.88 (t, J = 5.8 Hz, 3H). ^{13}C NMR (100 MHz, CHCl3): δ 150.19, 143.18, 128.85, 118.72, 31.83, 29.69, 29.31, 29.27, 29.18, 29.05, 22.67, 14.12.

2.4. Synthesis of 3,3′,3‴,3⁗′,3⁗″-quinqueoctyl-2,5′:2′,5″:2″,2‴:5‴,2⁗:5⁗′,2⁗″-sexithiophene (3)

TMEDA (0.10 ml, 0.69 mmol.) was added to a solution of quinquethiophene **1** (400 mg, 0.46 mmol) in anhydrous THF (20 ml) under Ar. The solution was cooled to −78 °C and *n*-BuLi in hexane (0.32 ml, 2.9 M, 0.92 mmol) was added dropwise. After stirring for 3 h at −78 °C, $ZnCl_2$ in diethyl ether (0.92 ml, 1 M, 0.92 mmol) was added to the stirred solution and the reaction mixture was stirred for 0.5 h and an additional 3 h after removing the cooling bath. In a second flask, 2-bromo-3-octyl-thiophene (139 mg, 0.51 mmol) and $Pd[PPh_3]_4$ (27 mg, 0.023 mmol) were stirred in THF (10 ml) for 10 min under Ar and then the solution was transferred to the zinc organic solution. The reaction was then shielded from light and allowed to proceed at 60 °C for 20 h. After cooling to room temperature, it was quenched with water and extracted with CH_2Cl_2 three times. The combined organic layer was washed

with H_2O and brine, dried over Na_2SO_4, and evaporated under reduced pressure. The crude was purified by column chromatography (silica, petroleum ether) to obtain sexithiophene **3** (224 mg, 0.21 mmol, 46%) as an orange solid. ^1H NMR (400 MHz, $CHCl_3$): 7.18 (d, J = 1.4 Hz, 1H), 7.17 (d, J = 1.4 Hz, 1H), 7.11 (s, 2H), 6.99 (s, 1H), 6.97 (s, 1H), 6.96 (s, 1H), 6.95 (s, 1H), 6.94 (s, 1H), 2.80 (m, 10H), 1.69 (m, 10H), 1.29 (m, 50H), 0.89 (m, 15H). ^{13}C NMR (100 MHz, $CHCl_3$): δ 139.90, 139.84, 139.81, 139.64, 139.60, 135.74, 135.67, 134.25, 134.09, 133.90, 130.48, 130.43, 130.27, 130.21, 130.09, 128.74, 128.54, 125.87, 123.60, 123.57, 31.90, 30.68, 30.63, 30.56, 29.62, 29.54, 29.48, 29.43, 29.29, 22.67, 14.12. HRMS (MALDI-FTICR): Calc. for $[M]^+$, 1054.5674; found, 1054.5669.

2.5. Synthesis of 5-nitro-3,3′,3″,3‴′,3⁗-quinqueoctyl-2,5′:2′,5″:2″,2‴:5‴,2‴′:5‴′, 2‴-sexithiophene (4)

TMEDA (0.78 ml, 5.21 mmol.) was added to a solution of quinquethiophene **1** (3.0 g, 3.47 mmol) in anhydrous THF (40 ml) under Ar. The solution was cooled to −78 °C and *n*-BuLi in hexane (2.7 ml, 2.9 M, 6.94 mmol) was added dropwise. After stirring for 3 h at −78 °C, $ZnCl_2$ in diethyl ether (6.94 ml, 1 M, 6.94 mmol) was added to the stirred solution and the reaction mixture was stirred for 0.5 h and an additional 3 h after removing the cooling bath. In a second flask, 2-bromo-3-octyl-5-nitrothiophene (1.22 g, 3.82 mmol) and $Pd[PPh_3]_4$ (160 mg, 0.14 mmol) were stirred in THF (20 ml) for 10 min under Ar and then the solution was transferred to the zinc organic solution. The reaction was then shielded from light and allowed to proceed at 60 °C for 20 h. After cooling to room temperature, it was quenched with water and extracted with CH_2Cl_2 three times. The combined organic layer was washed with H_2O and brine, dried over Na_2SO_4, and evaporated under reduced pressure. The crude was purified by column chromatography (silica, petroleum ether–CH_2Cl_2 5:1) to obtain nitrosexithiophene **4** (1.57 g, 1.43 mmol, 41%) as a puce solid. ^1H NMR (400 MHz, $CHCl_3$): 7.76 (s, 1H), 7.17 (d, J = 5.2 Hz, 1H), 7.12 (s, 1H), 7.11 (s, 1H), 7.10 (s, 1H), 7.02 (s, 1H), 6.96 (s, 1H), 6.94 (d, J = 5.2 Hz, 1H), 2.80 (m, 10H), 1.68 (m, 10H), 1.28 (m, 50H), 0.88 (m, 15H). ^{13}C NMR (100 MHz, $CHCl_3$): δ 147.96, 140.35, 140.12, 140.02, 139.74, 139.38, 138.95, 136.24, 135.23, 134.46, 133.83, 132.77, 131.5, 131.23, 131.14, 131.03, 130.39, 130.13, 130.05, 129.38, 128.79, 126.22, 125.94, 123.71, 31.90, 31.85, 30.70, 30.62, 30.50, 30.09, 29.62, 29.53, 29.48, 29.42, 29.32, 29.29, 29.21, 22.69, 14.12. HRMS (MALDI-FTICR): Calc. for $[M]^+$, 1099.5531; found, 1099.5532.

2.6. Synthesis of 5-amino-3,3’,3”,3‴,3⁗-quinqueoctyl-2,5’:2’,5”:2”,2‴:5‴,2⁗:5⁗,2⁗′-sexithiophene (5)

Nitrosexithiophene **4** (480 mg, 0.44 mmol) was dissolved in ethyl acetate (35 mL) and 10% Pd/C (320 mg) was added. After two vacuum/H_2 cycles to replace the air inside with hydrogen, the mixture was vigorously stirred at room temperature (ca. 20 °C) under ordinary hydrogen pressure (balloon) for 24 h. The reaction mixture was filtered through Celite and the filtrate was concentrated and dried under vacuum to provide the product. The product was used directly in the next step without further purification.

2.7. Synthesis of 6THIOP-NH-SPFGraphene

A mixture of graphene oxide (60 mg), 6THIOP-NH_2 (400 mg) and 1,3-diisopropylcarbodiimide (DIC, 0.6 ml) were mixed with ODCB (40 ml) in a 100 ml round-bottomed flask and heated to 80 °C for 48 h under Ar and an additional 6 h with intermittent sonication to give a homogeneous black dispersion. After the reaction, the solution was cooled to room temperature, and then poured into ethanol (300 ml) to precipitate the product. The precipitate was collected by centrifuge at 8000 rpm for 0.5 h. The supernatant which contained dissolved DIC was discarded. To wash the precipitate thoroughly, another 100 ml ethanol was added, the mixture was sonicated for 5 min and then centrifuged at 8000 rpm for 0.5 h to collect the 6THIOP-NH-SPFGraphene, discarding the supernatant. The precipitate was washed with ethanol five times again and then with toluene five times following the above procedure. UV–Vis spectra and thin layer chromatography (TLC) were used to check the supernatant layer to ensure no 6THIOP-NH_2 existed in the final washing. At last, 50 ml toluene was added to the black centrifugate and the product was isolated by filtration on a Nylon membrane (0.22 μm) and then the product was dried under vacuum to yield the hybrid 6THIOP-NH-SPFGraphene (71 mg).

3. Results and discussion

3.1. Synthesis of the materials

The synthesis route for functionalized graphene, 6THIOP-NH-SPFGraphene, is summarized in Fig. 1. The starting materials, quinquethiophene **1**, were synthesized according to the literature [41]. Oligothiophenes **3** and **4** were prepared similarly by utilizing Negishi cross-coupling reaction [42]. Because of the unstable properties of aminothiophenes [43], the nitrosexithiophene **4** was reduced to 6THIOP-NH_2 by hydrogenation in the presence of Pd/C and the product was used directly in the next step without further purification.

The synthesis of oligothiphene-graphene nanohybrid, 6THIOP-NH-SPFGraphene (Figs. 1 and 2), was carried out using an amine functionalized oligothiophene (6THIOP-NH_2) and graphene oxide in ODCB following a general synthetic methodology. The oligothiophene and graphene in the hybrid 6THIOP-NH-SPFGraphene act as a donor and acceptor, respectively. Large scale and water soluble graphene oxide was prepared by the modified Hummers method [15,44,45]. Results of atomic force microscopy (AFM), TGA and X-ray diffraction (XRD) characterization have confirmed that this graphene material can be easily dispersed at the state of complete exfoliation consisting of almost entire single-layered graphene sheets in H_2O [15,44]. 6THIOP-NH_2 and graphene oxide molecules are covalently bonded together using amide bond. Much care has been taken to make sure all the unreacted 6THIOP-NH_2 has been removed by repeated centrifugation and redispersion, and then membrane filtration and washing. The covalent functionalization of graphene oxide with oligothiophenes has changed graphene oxide from hydrophilic to hydrophobic and the hybrid can be dissolved in organic solvents such as ODCB. This makes it

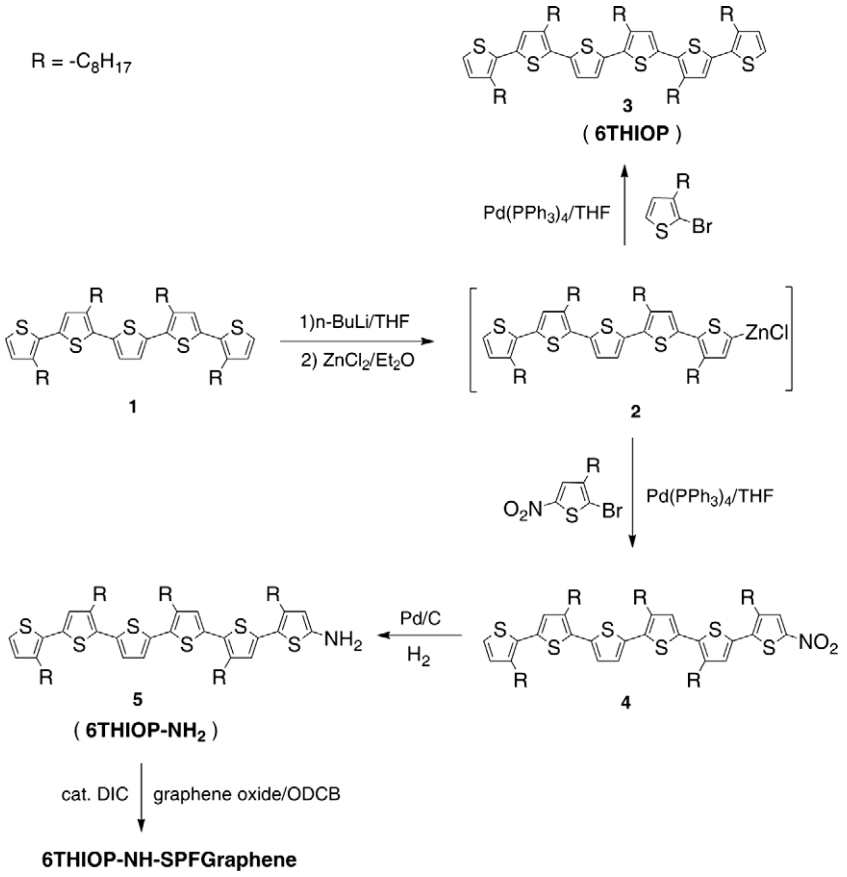

Fig. 1 – Synthesis route to 6THIOP-NH-SPFGraphene.

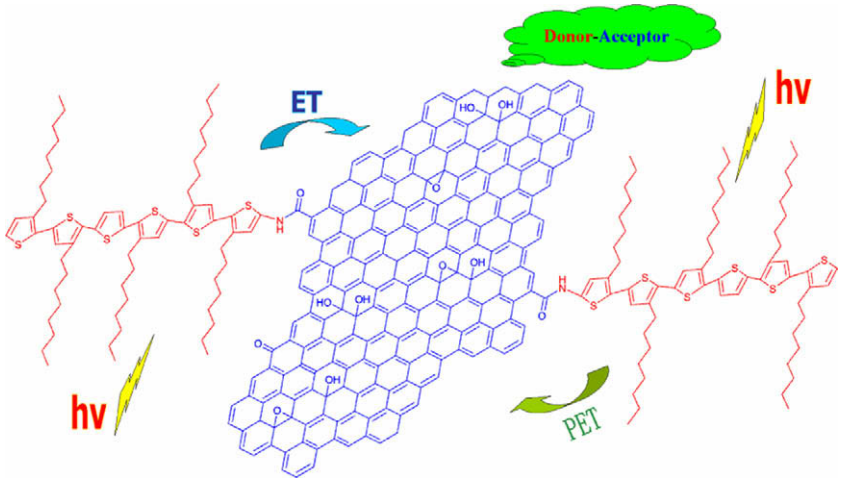

Fig. 2 – Structure of 6THIOP-NH-SPFGraphene.

possible that this graphene hybrid can be homogeneously dispersed (together with other organic materials) in organic solvents needed for various organic electronic applications. Using elemental analysis, the weight fractions of C, H, N, and S of the 6THIOP-NH-SPFGraphene were determined to be 67.42%, 5.42%, 0.49% and 6.27%. Based on this, it is estimated that the ratio of the oligomer chain (6THIOP) with the carbon atoms on graphene is ~1/108.

3.2. *Solid-state NMR structural characterization*

The ^{13}C CP/MAS NMR spectra of graphene oxide and 6THIOP-NH-SPFGraphene (Fig. 3) indicate significant structural change induced by the functionlization of graphene with oligothiophene. In the spectrum of grapheme oxide, the peaks at 61.4 and 71.7 ppm represent the ^{13}C nuclei in the epoxide and hydroxyl groups, respectively [46,47]. The resonance at

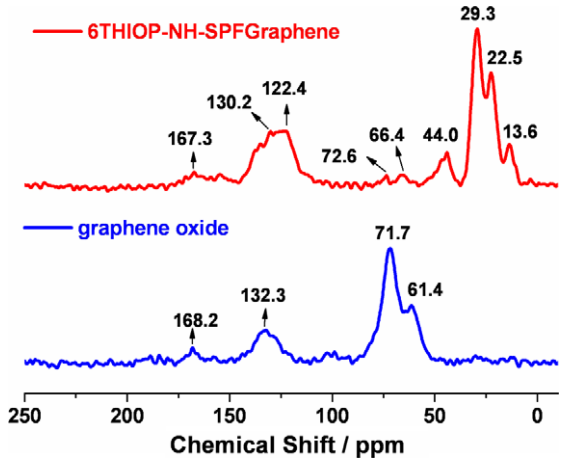

Fig. 3 – ^{13}C CP/MAS NMR spectra with ^{1}H decoupling of graphene oxide and 6THIOP-NH-SPFGraphene.

132.3 ppm belongs to the un-oxidized sp^2 carbons of the graphene network and that at 168.2 ppm presumably arises from the carbonyl groups [46,47]. In the ^{13}C NMR spectrum of 6THIOP-NH-SPFGraphene, the peaks of the ^{13}C nuclei in the epoxide and hydroxyl groups are weak, like the deoxygenation of graphene oxide under alkaline conditions [48], this can be attributed to the strong dehydration capacity of DIC. The new peaks from 13.6 to 44.0 ppm can be attributed to the alkyl of oligothiophenes. The peaks around 130 ppm are broadened because the new sp^2 carbons from oligothiophenes are introduced. These results clearly indicate that the new graphene-based materials are formed.

3.3. *Thermal and optical properties*

Fig. 4 shows FTIR spectra of 6THIOP-NH-SPFGraphene, 6THIOP, and the graphene oxide. The most characteristic features

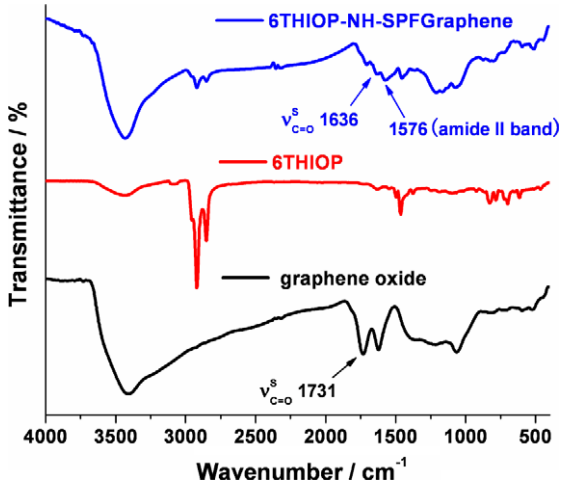

Fig. 4 – FTIR spectra of 6THIOP-NH-SPFGraphene, 6THIOP and graphene oxide. The peak at 1636 cm^{-1}, corresponding to the C=O stretch of the amide group, indicating that the oligothiophene molecules have been covalently bonded to the graphene oxide via the amide linkage.

of graphene oxide in the FTIR spectra are the characteristic C=O stretch of the carboxylic group at 1731 cm^{-1}. The band present at 1622 cm^{-1} is attributed to the deformations of the O–H bond of the strongly intercalated water absorbed by graphene oxide, but may also contains the stretch of aromatic C=C bond [16,18,49]. Deformation of the C-O bond is observed as the intense band present at 1064 cm^{-1}. After covalent functionalization with oligothiophene, the peak of deformation of the C–O bond shifts to 1072. The peak present at 1454 is assigned to the bending vibration of CH_2. The new peak at 1643 cm^{-1} in the spectrum of 6THIOP-NH-SPFGraphene corresponds to the amide I band, which is carbonyl stretching of the amide. The peak at 1576 cm^{-1} can be attributed to the amide II band, which is the coupling of the C–N stretching with the N-H deformation vibration [16]. We also observed the asymmetric C-H stretch at 2919 cm^{-1} and symmetric C–H stretch at 2849 cm^{-1} of the alkyl groups. These results clearly indicated that the 6THIOP-NH_2 molecules had been covalently bonded to the graphene oxide via the amide linkage.

Fig. 5 shows Raman spectra of graphene oxide and 6THIOP-NH-SPFGraphene. The graphene oxide shows an intense tangential mode (G band) at 1594 cm^{-1}, with a disordered-induced peak (D band) at 1362 cm^{-1}. The 6THIOP-NH-SPFGraphene nanohybrid mainly shows three peaks at 1589, 1372 and 1449 cm^{-1}. The peak at 1449 cm^{-1} should be assigned to the CH_2 scissoring mode of the alkyl of oligothiophene. Comparing with the graphene oxide, the peaks at 1589 and 1372 cm^{-1} can be attributed to the G and D bands of the graphene sheets, which are shifted by 5 and 10 cm^{-1}, respectively. This relatively large shift sufficiently suggests a strong interaction between the oligothiophene molecules and the graphene sheets.

The thermal behaviors of the graphene oxide and 6THIOP-NH-SPFGraphene hybrid were investigated by TGA under nitrogen atmosphere (Fig. 6). The initial weight loss of graphene oxide below 150 °C is 13%, which is ascribed to the elimination of adsorbed water. The weight loss (5%) of 6THIOP-NH-SPFGraphene below 150 °C, much smaller than that for graphene oxide, could be due to adsorbed solvent too [50]. A large weight loss around 200 °C owes to the removal

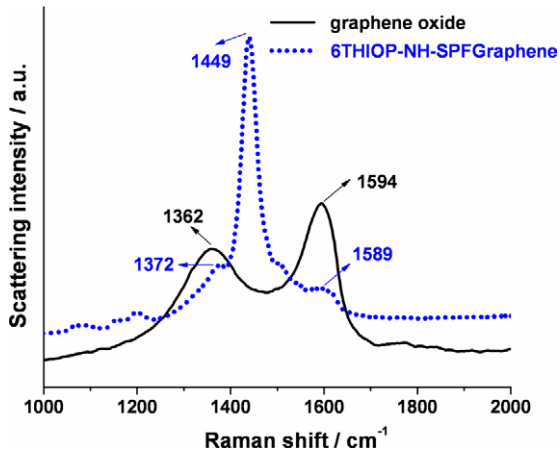

Fig. 5 – Raman spectra of graphene oxide and 6THIOP-NH-SPFGraphene excited at 514 nm.

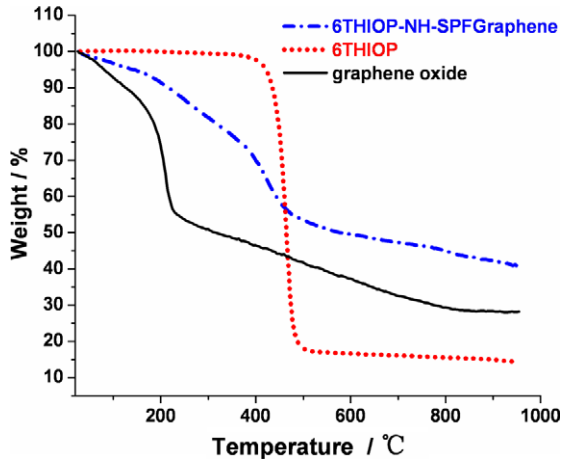

Fig. 6 – TGA curves of 6THIOP-NH-SPFGraphene, 6THIOP and graphene oxide. The 6THIOP-NH-SPFGraphene hybrid shows increased onset temperature compared with graphene oxide, indicating that new chemical bonds are formed between the graphene sheet and oligothiophene.

of the oxygen functional groups from the graphene oxide layers [46,51]. In this stage, graphene oxide loses 34% of its weight, and the 6THIOP-NH-SPFGraphene hybrid loses only 10%. For the 6THIOP, a weight loss of 83% occurred at an onset temperature of 444 °C, which is due to the decomposition of the organic functional groups. The 6THIOP-NH-SPFGraphene hybrid shows a mass loss, starting at an onset temperature of 386 °C, illustrating the oxidative decomposition of the organic functional groups and further carbonization of the graphene backbone [52,53]. The increased onset temperature of the 6THIOP-NH-SPFGraphene compared with its parent graphene oxide indicate that new chemical bonds are formed and oligothiophenes are chemically bonded onto graphene sheets. These results indicate that the 6THIOP-NH-SPFGraphene hybrid is thermally more stable than graphene oxide.

Fig. 7 shows UV–Vis absorption spectra of 6THIOP-NH-SPFGraphene, 6THIOP and graphene oxide. The spectra of 6THIOP-NH-SPFGraphene and 6THIOP were observed in the ODCB solution and that of graphene oxide in water. The spectra are plotted in the wavelength range from 300 to 800 nm because of the impossibility of properly compensating for the strong absorption of ODCB at shorter wavelength. Graphene oxide shows a broad absorption with continuously decreasing intensity ranged to 800 nm. The 6THIOP shows a strong broad π-π^* absorption band at 411 nm. 6THIOP-NH-SPFGraphene shows an absorption band at around 412 nm, derived from the oligothiophene group, and has a very broad absorption in the whole spectral region, which suggests a charge-transfer interaction between the oligothiophene and graphene units [21,37].

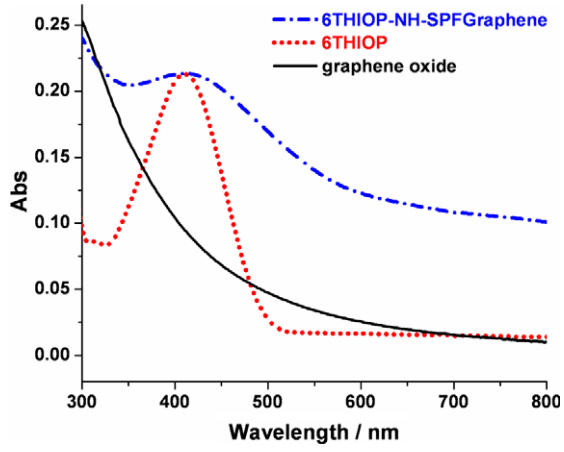

Fig. 7 – UV–Vis absorption spectra of graphene oxide (5.9 mg L^{-1}) in aqueous solution, 6THIOP (3.0 mg L^{-1}) and 6THIOP-NH-SPFGraphene (3.8 mg L^{-1}) in ODCB.

The prevention of aggregation is of particular importance for graphene processability and applications because most of their attractive properties are only associated with individual graphene sheets. Solution-phase UV–Vis spectroscopy has been reported to demonstrate a linear relationship between the absorbance and the relative concentrations of functionalized graphene in THF, obeying Beer's law at low concentrations, and has been used to determine the solubility of functionalized graphene [54]. Fig. 8 shows the absorption spectra of solutions of 6THIOP-NH-SPFGraphene with different concentrations. The absorption values at 412 nm were plotted against concentrations as shown in Fig. 8. Applying the Beer's law, we estimated the effective extinction coefficient of the 6THIOP-NH-SPFGraphene from the slope of the linear least-squares fit to be 0.041 L mg^{-1} cm^{-1}, with an R value of 0.999. The absorbance of solutions of 6THIOP-NH-SPFGraphene at other wavelengths were in line with the Beer's law too. These linear relationship results demonstrated that the hybrid had been homogeneously dispersed in the ODCB.

In order to probe excited-state interactions of graphene and oligothiophene in the hybrid, fluorescence spectra of 6THIOP-NH-SPFGraphene and 6THIOP were compared in

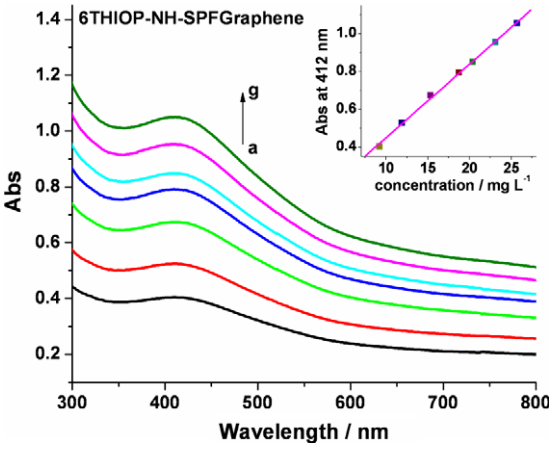

Fig. 8 – Concentration dependence of UV–Vis absorption spectra of 6THIOP-NH-SPFGraphene in ODCB (concentrations are 9.2, 11.9, 15.3, 18.7, 20.4, 23.1 and 25.7 mg L^{-1}, from *a–g*, respectively). Shown in the insets are the plots of optical density at 412 nm versus concentration. The straight lines are a linear least-squares fit to the data, indicating the hybrid 6THIOP-NH-SPFGraphene was dissolved homogeneously in the solvent.

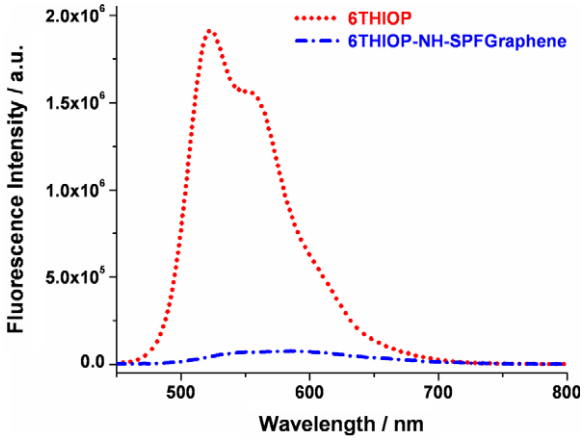

Fig. 9 – Fluorescence spectra of 6THIOP-NH-SPFGraphene (λ_{ex} = 411 nm) and 6THIOP (λ_{ex} = 411 nm) in ODCB with the same absorbance value (Abs = 0.21).

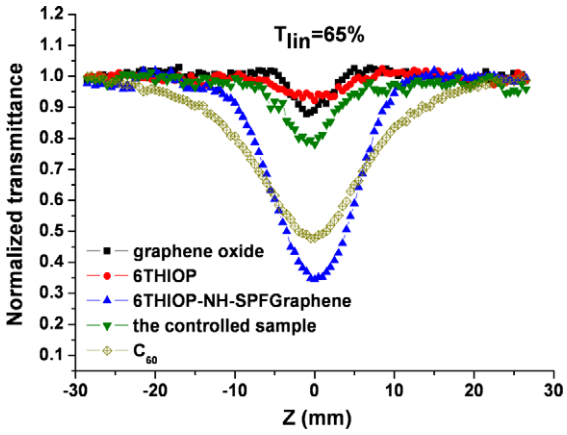

Fig. 10 – Open-aperture Z-scan results of 6THIOP-NH-SPFGraphene, 6THIOP, graphene oxide, the controlled sample (6THIOP and graphene oxide), and C_{60} with the same linear transmittance of 65% to 5 ns, 532 nm optical pulses.

Fig. 9. Upon excitation at 411 nm, the solution of 6THIOP-NH-SPFGraphene exhibits about 98% quenching of the fluorescence emission bands at 522 nm, as compared to that of 6THIOP at a matching absorption (0.21). The observed almost completely luminescence quenching indicated that there was a strong interaction between the excited state of 6THIOP and graphene moieties in the hybrid. Possible pathways for the fluorescence quenching of the excited 6THIOP may be attributed to two possible competitive processes: photoinduced electron transfer (PET) and energy transfer (ET). Similar luminescence quenching has been observed for the hybrids of C_{60} with oligothiophene and PET and ET mechanism has been demonstrated for these hybrids [55–57]. Molecular orbital theory and experimental results have shown that closed-cage carbon structures such as fullerenes and carbon nanotubes are favorable electron acceptors because of their unique π-electron system when the two moieties are connected directly [58]. Thus, after photoexcitation, the intramolecular donor–acceptor interaction between the two moieties of oligothiophene and graphene in our 6THIOP-NH-SPFGraphene nanohybrid may have a charge transfer from the photoexcited singlet oligothiophene to graphene moiety, and this results in the observed fluorescence quenching and energy releasing.

3.4. *Optical limiting properties*

Dipolar push–pull chromophores with C_{60} and carbon nanotubes derivatives as acceptor have excellent optical limiting properties with the efficient energy and/or electron transfer upon photoexcitation [32,59–61]. It would be both interesting and important to investigate the optical limiting properties of the 6THIOP-NH-SPFGraphene hybrid. Optical limiters are materials that strongly attenuate intense optical beams, potentially dangerous optical beams, while exhibiting high transmittance for low-intensity ambient light levels. They can be used for the protection of human eyes, optical elements and optical sensors from intense laser pulses.

Fig. 10 shows open-aperture Z-scan [62] results of 6THIOP-NH-SPFGraphene (in ODCB), 6THIOP-NH_2 (in ODCB), graphene oxide (in DMF), a controlled blend sample (1:1, v/v) of 6THIOP (in ODCB) with graphene oxide (in DMF) and C_{60} (in toluene). Because of the poor solubility of graphene oxide in ODCB, a component (ODCB and DMF) solvent in the controlled blend sample was used. The optical limiting properties of the solutions of these materials were investigated using 532 nm pulsed laser irradiation, and C_{60} was employed as a standard. To compare the optical limiting effect, all of the sample concentrations were adjusted to have the same linear transmittance of 65% at 532 nm in 1-mm-thick cells.

The open-aperture Z-scan measures the transmittance of sample as it translates through the focal plane of a tightly focused beam. As the sample is brought closer to focus, the beam intensity increases and nonlinear effect increases, which will lead to a decreasing transmittance for two-photon absorption (TPA) and nonlinear scattering. As shown in Fig. 10, the 6THIOP-NH-SPFGraphene had the largest dip among the transmittance curves of the studied materials: 6THIOP-NH-SPFGraphene, 6THIOP, graphene oxide, the controlled sample and C_{60}. Therefore, 6THIOP-NH-SPFGraphene demonstrated much better optical limiting properties compared with the controlled blend sample and the individual components (6THIOP and graphene oxide) of the hybrid, and even better than the benchmark material C_{60}. Graphene oxide may have TPA while using 532 nm pulsed laser irradiation in our experiments because the linear absorption peak of graphene oxide below 300 nm [63]. Considering the covalent donor–acceptor structure and the efficient fluorescence quenching of this nanohybrid above, we believe that the PET and/or ET from electron donor 6-THIOP to acceptor graphene should play an important role for the much-enhanced optical limiting performance [61]. Furthermore, in the process of Z-scan experiments as shown in Fig. 10, enhanced scattering could be also observed for the sample of 6THIOP-NH-SPFGraphene moving towards the focus of the laser. This implied that the observed Z-scan curve was also influenced by nonlinear scattering. Therefore, the much-enhanced optical limiting performance of 6THIOP-NH-SPFGraphene should arise from a

combination of PET and/or ET, TPA and nonlinear scattering mechanisms. Similar results have been observed the hybrid materials of carbon nanotubes and graphene with porphyrins [31,32,63].

4. Conclusions

We have reported the first covalently bonded and organic soluble graphene hybrid with oligothiophenes. Solid ^{13}C NMR, FTIR and Raman spectra confirmed the covalent functionalization of graphene. Attachment of oligothiophenes significantly improved its solubility and dispersion stability of the graphene-based material in organic solvents. In this donor–acceptor nanohybrid, fluorescence of photoexcited 6THIOP was effectively quenched through a possible PET and/or ET process. A superior optical limiting effect, better than the benchmark optical limiting material C_{60} and the controlled sample was observed. PET and/or ET mechanism is believed to play a significant role for its superior optical limiting performance. With the abundant and highly pure functionalized graphene material readily available, unique structure and excellent electronic properties, we fully expect this organic solution-processable functionalized graphene material may bring a competitive entry into the realm of light harvesting and solar energy conversion materials for optoelectronic devices, which is current underway.

Acknowledgments

The authors gratefully acknowledge the financial support from the NSFC (#20774047), MOST (#2006CB932702), MOE (#708020) of China and NSF of Tianjin City (#07JCYBJC03000 and #08JCZDJC25300).

REFERENCES

[1] Eda G, Fanchini G, Chhowalla M. Large-area ultrathin films of reduced graphene oxide as a transparent and flexible electronic material. Nat Nanotechnol 2008;3(5):270–4.
[2] Geim AK, Novoselov KS. The rise of graphene. Nat Mater 2007;6(3):183–91.
[3] Novoselov KS, Jiang Z, Zhang Y, Morozov SV, Stormer HL, Zeitler U, et al. Room-temperature quantum hall effect in graphene. Science 2007;315(5817):1379.
[4] Mak KF, Sfeir MY, Wu Y, Lui CH, Misewich JA, Heinz TF. Measurement of the optical conductivity of graphene. Phys Rev Lett 2008;101(19):196405-1–4.
[5] Wang F, Zhang YB, Tian CS, Girit C, Zettl A, Crommie M, et al. Gate-variable optical transitions in graphene. Science 2008;320(5873):206–9.
[6] Nomura K, MacDonald AH. Quantum Hall ferromagnetism in graphene. Phys Rev Lett 2006;96(25):256602-1–4.
[7] Wang Y, Huang Y, Song Y, Zhang XY, Ma YF, Liang JJ, et al. Room-temperature ferromagnetism of graphene. Nano Lett 2009;9(1):220–4.
[8] Dikin DA, Stankovich S, Zimney EJ, Piner RD, Dommett GHB, Evmenenko G, et al. Preparation and characterization of graphene oxide paper. Nature 2007;448(7152):457–60.
[9] Lee C, Wei XD, Kysar JW, Hone J. Measurement of the elastic properties and intrinsic strength of monolayer graphene. Science 2008;321(5887):385–8.
[10] Tasis D, Tagmatarchis N, Bianco A, Prato M. Chemistry of carbon nanotubes. Chem Rev 2006;106(3):1105–36.
[11] Martin N, Sanchez L, Illescas B, Perez I. C-60-based electroactive organofullerenes. Chem Rev 1998;98(7):2527–47.
[12] Gilje S, Han S, Wang M, Wang KL, Kaner RB. A chemical route to graphene for device applications. Nano Lett 2007;7(11):3394–8.
[13] Stoller MD, Park SJ, Zhu YW, An JH, Ruoff RS. Graphene-based ultracapacitors. Nano Lett 2008;8(10):3498–502.
[14] Schedin F, Geim AK, Morozov SV, Hill EW, Blake P, Katsnelson MI, et al. Detection of individual gas molecules adsorbed on graphene. Nat Mater 2007;6(9):652–5.
[15] Liu ZF, Liu Q, Huang Y, Ma YF, Yin SG, Zhang XY, et al. Organic photovoltaic devices based on a novel acceptor material: graphene. Adv Mater 2008;20(20):3924–30.
[16] Stankovich S, Piner RD, Nguyen ST, Ruoff RS. Synthesis and exfoliation of isocyanate-treated graphene oxide nanoplatelets. Carbon 2006;44(15):3342–7.
[17] Stankovich S, Dikin DA, Dommett GHB, Kohlhaas KM, Zimney EJ, Stach EA, et al. Graphene-based composite materials. Nature 2006;442(7100):282–6.
[18] Si Y, Samulski ET. Synthesis of water soluble graphene. Nano Lett 2008;8(6):1679–82.
[19] Wang S, Chia PJ, Chua LL, Zhao LH, Png RQ, Sivaramakrishnan S, et al. Band-like transport in surface-functionalized highly solution-processable graphene nanosheets. Adv Mater 2008;20(18):3440–6.
[20] Murphy AR, Frechet JMJ, Chang P, Lee J, Subramanian V. Organic thin film transistors from a soluble oligothiophene derivative containing thermally removable solubilizing groups. J Am Chem Soc 2004;126(6):1596–7.
[21] Li WS, Yamamoto Y, Fukushima T, Saeki A, Seki S, Tagawa S, et al. Amphiphilic molecular design as a rational strategy for tailoring bicontinuous electron donor and acceptor arrays: photoconductive liquid crystalline oligothiophene-C-60 dyads. J Am Chem Soc 2008;130(28):8886–7.
[22] Yamada R, Kumazawa H, Noutoshi T, Tanaka S, Tada H. Electrical conductance of oligothiophene molecular wires. Nano Lett 2008;8(4):1237–40.
[23] Schulze K, Uhrich C, Schuppel R, Leo K, Pfeiffer M, Brier E, et al. Efficient vacuum-deposited organic solar cells based on a new low-bandgap oligothiophene and fullerene C-60. Adv Mater 2006;18(21):2872–5.
[24] Cravino A, Roquet S, Aleveque O, Leriche P, Frere P, Roncali J. Triphenylamine–oligothiophene conjugated systems as organic semiconductors for opto-electronics. Chem Mater 2006;18(10):2584–90.
[25] Breitung EM, Shu CF, McMahon RJ. Thiazole and thiophene analogues of donor-acceptor stilbenes: molecular hyperpolarizabilities and structure-property relationships. J Am Chem Soc 2000;122(6):1154–60.
[26] Waite J, Papadopoulos MG. The effect of charge transfer on the polarizability and hyperpolarizabilities of some selected, substituted polythiophenes: a comparative study. J Phys Chem 1990;94:6244–9.
[27] Raimundo JM, Blanchard P, Gallego-Planas N, Mercier N, Ledoux-Rak I, Hierle R, et al. Design and synthesis of push-pull chromophores for second-order nonlinear optics derived from rigidified thiophene-based pi-conjugating spacers. J Org Chem 2002;67(1):205–18.
[28] Videlot-Ackermann C, Isoshima T, Yassar A, Wada T, Sasabe H, Fichou D. Third-order nonlinear optical properties of oligothiophene-based thin films investigated by electro absorption spectroscopy: influence of conjugated chain

length and electron-withdrawing substituents. Synth Met 2006;156(2–4):154–61.
[29] Brasselet S, Cherioux F, Audebert P, Zyss J. New octupolar star-shaped structures for quadratic nonlinear optics. Chem Mater 1999;11(7):1915–20.
[30] Ramakrishna G, Bhaskar A, Bauerle P, Goodson T. Oligothiophene dendrimers as new building blocks for optical applications. J Phys Chem A 2008;112(10):2018–26.
[31] Liu ZB, Tian JG, Guo Z, Ren DM, Du T, Zheng JY, et al. Enhanced optical limiting effects in porphyrin-covalently functionalized single-walled carbon nanotubes. Adv Mater 2008;20(3):511–5.
[32] Guo Z, Du F, Ren DM, Chen YS, Zheng JY, Liu ZB, et al. Covalently porphyrin-functionalized single-walled carbon nanotubes: a novel photoactive and optical limiting donor-acceptor nanohybrid. J Mater Chem 2006;16(29):3021–30.
[33] Priyadarshy S, Therien MJ, Beratan DN. Acetylenyl-linked, porphyrin-bridged, donor-acceptor molecules: a theoretical analysis of the molecular first hyperpolarizability in highly conjugated push–pull chromophore structures. J Am Chem Soc 1996;118(6):1504–10.
[34] Wu XM, Wu JY, Liu YQ, Jen AKY. Highly efficient, thermally and chemically stable nonlinear optical chromophores based on the alpha-perfluoroaryldicyanovinyl electron acceptors. Chem Commun 1999(23):2391–2.
[35] Jen AKY, Liu YQ, Zheng LX, Liu S, Drost KJ, Zhang Y, et al. Synthesis and characterization of highly efficient, chemically and thermally stable chromophores with chromone-containing electron acceptors for NLO applications. Adv Mater 1999;11(6):452–5.
[36] Cremer J, Bauerle P. Star-shaped perylene–oligothiophene–triphenylamine hybrid systems for photovoltaic applications. J Mater Chem 2006;16(9):874–84.
[37] Tamayo AB, Walker B, Nguyen TQ. A low band gap, solution processable oligothiophene with a diketopyrrolopyrrole core for use in organic solar cells. J Phys Chem C 2008;112(30):11545–51.
[38] Negishi N, Takimiya K, Otsubo T, Harima Y, Aso Y. Oligothiophene-multifullerene linkage molecules as high performance photovoltaic materials. Synth Met 2005;152(1–3):125–8.
[39] Guldi DM, Rahman GMA, Zerbetto F, Prato M. Carbon nanotubes in electron donor-acceptor nanocomposites. Acc Chem Res 2005;38(11):871–8.
[40] Nishizawa T, Tajima K, Hashimoto K. The effect of crystallinity in donor groups on the performance of photovoltaic devices based on an oligothiophene–fullerene dyad. Nanotechnology 2008;19(42):424017-1–8.
[41] Liu YS, Zhou JY, Wan XJ, Chen YS. Synthesis and properties of acceptor–donor–acceptor molecules based on oligothiophenes with tunable and low band gap. Tetrahedron 2009;65(27):5209–15.
[42] Ibrahim MA, Lee BG, Park NG, Pugh JR, Eberl DD, Frank AJ. Synthesis of new oligothiophene derivatives and their intercalation compounds: orientation effects. Synth Met 1999;105(1):35–42.
[43] Stacy GW, Eck DL. 2-Aminothiophene. Heterocyclization of benzylthionitriles. Tetrahedron Lett 1967;8(51):5201–4.
[44] Becerril HA, Mao J, Liu Z, Stoltenberg RM, Bao Z, Chen Y. Evaluation of solution-processed reduced graphene oxide films as transparent conductors. Acs Nano 2008;2(3):463–70.
[45] Hummers WS, Offeman RE. Preparation of graphitic oxide. J Am Chem Soc 1958;80(6):1339.
[46] Lerf A, He HY, Forster M, Klinowski J. Structure of graphite oxide revisited. J Phys Chem B 1998;102(23):4477–82.
[47] Cai WW, Piner RD, Stadermann FJ, Park S, Shaibat MA, Ishii Y, et al. Synthesis and solid-state NMR structural characterization of C-13-labeled graphite oxide. Science 2008;321(5897):1815–7.
[48] Fan XB, Peng WC, Li Y, Li XY, Wang SL, Zhang GL, et al. Deoxygenation of exfoliated graphite oxide under alkaline conditions: a green route to graphene preparation. Adv Mater 2008;20(23):4490–3.
[49] Park S, Lee KS, Bozoklu G, Cai W, Nguyen ST, Ruoff' RS. Graphene oxide papers modified by divalent ions – enhancing mechanical properties via chemical cross-linking. Acs Nano 2008;2(3):572–8.
[50] Wang GC, Yang ZY, Li XW, Li CZ. Synthesis of poly(aniline-co-o-anisidine)-intercalated graphite oxide composite by delamination/reassembling method. Carbon 2005;43(12):2564–70.
[51] Stankovich S, Dikin DA, Piner RD, Kohlhaas KA, Kleinhammes A, Jia Y, et al. Synthesis of graphene-based nanosheets via chemical reduction of exfoliated graphite oxide. Carbon 2007;45(7):1558–65.
[52] Wang ZM, Shishibori K, Hoshinoo K, Kanoh H, Hirotsu T. Examination of synthesis conditions for graphite-derived nanoporous carbon–silica composites. Carbon 2006;44(12):2479–88.
[53] Niyogi S, Bekyarova E, Itkis ME, McWilliams JL, Hamon MA, Haddon RC. Solution properties of graphite and graphene. J Am Chem Soc 2006;128(24):7720–1.
[54] Muszynski R, Seger B, Kamat PV. Decorating graphene sheets with gold nanoparticles. J Phys Chem C 2008;112(14):5263–6.
[55] van Hal PA, Knol J, Langeveld-Voss BMW, Meskers SCJ, Hummelen JC, Janssen RAJ. Photoinduced energy and electron transfer in fullerene–oligothiophene–fullerene triads. J Phys Chem A 2000;104(25):5974–88.
[56] Narutaki M, Takimiya K, Otsubo T, Harima Y, Zhang HM, Araki Y, et al. Synthesis and photophysical properties of two dual oligothiophene-fullerene linkage molecules as photoinduced long-distance charge separation systems. J Org Chem 2006;71(5):1761–8.
[57] Nakamura T, Araki Y, Ito O, Takimiya K, Otsubo T. Fluorescence up-conversion study of excitation energy transport dynamics in oligothiophene–fullerene linked dyads. J Phys Chem A 2008;112(6):1125–32.
[58] Fowler PW, Ceulemans A. Electron deficiency of the fullerenes. J Phys Chem 1995;99(2):508–10.
[59] Senge MO, Fazekas M, Notaras EGA, Blau WJ, Zawadzka M, Locos OB, et al. Nonlinear optical properties of porphyrins. Adv Mater 2007;19(19):2737–74.
[60] Zhu PW, Wang P, Qiu WF, Liu YQ, Ye C, Fang GY, et al. Optical limiting properties of phthalocyanine–fullerene derivatives. Appl Phys Lett 2001;78(10):1319–21.
[61] Wu W, Zhang S, Li Y, Li JX, Liu LQ, Qin YJ, et al. PVK-modified single-walled carbon nanotubes with effective photoinduced electron transfer. Macromolecules 2003;36(17):6286–8.
[62] Sheikbahae M, Said AA, Wei TH, Hagan DJ, Vanstryland EW. Sensitive measurement of optical nonlinearities using a single beam. IEEE J Quantum Electron 1990;26(4):760–9.
[63] Xu YF, Liu ZB, Zhang XL, Wang Y, Tian JG, Huang Y, et al. a graphene hybrid material covalently functionalized with porphyrin: synthesis and optical limiting property. Adv Mater 2009:1275–9.